

Mapping Environmental Suitability for Malaria Transmission, Greece

Bertrand Sudre, Massimiliano Rossi,
Wim Van Bortel, Kostas Danis, Agoritsa Baka,
Nikos Vakalis, and Jan C. Semenza

During 2009–2012, Greece experienced a resurgence of domestic malaria transmission. To help guide malaria response efforts, we used spatial modeling to characterize environmental signatures of areas suitable for transmission. Nonlinear discriminant analysis indicated that sea-level altitude and land-surface temperature parameters are predictive in this regard.

Malaria was eliminated in Greece in 1974 (1,2); however, cases continue to be imported from countries to which malaria is endemic (3) and locally acquired cases have occurred sporadically (4,5). During 2009–2012, health authorities in Greece recorded 267 malaria cases. Although most cases were imported, at least 69 (26%) occurred in patients who did not have travel histories to malaria-endemic regions. A cluster of 6 locally acquired *Plasmodium vivax* malaria cases occurred during August–October 2009 in the southern Peloponnese (Evrotas Municipality, Lakonia district); in addition, 1 autochthonous case was reported from Marathon Municipality, East Attiki district (2). In 2010, locally transmitted cases were recorded in the same Lakonia district, 1 in East Attiki and 2 in children in central Greece (Viotia district). In 2011, a total of 42 autochthonous cases of *P. vivax* malaria were reported, representing 44% of the 96 notified cases in 2011. Most (36) of those cases were notified in the Evrotas municipality. In 2012, locally acquired cases appeared to have decreased, with 16 cases representing 21% of the overall number of cases. The ongoing transmission of *P. vivax* by local anopheline mosquitoes raises concern about reemergence of malaria transmission

in Greece in areas that are hospitable to the vector and have permissive environmental and climatic conditions (6).

The Study

To guide malaria control efforts, we delineated areas suitable for malaria transmission in Greece using the place of exposure for 69 locally acquired malaria cases. A health officer administered a standardized questionnaire to each malaria case-patient in Greece to determine the origin of infection. Our analysis was restricted to cases classified as locally acquired in persons without travel histories to optimize the specificity of the model because our goal was to describe the environmental suitability of autochthonous malaria transmission in Greece. Thus, our analysis excluded cases that might have been acquired abroad.

We aimed to describe the environmental profile of areas with active transmission cycles during 2009–2012 and then to predict other areas at risk for malaria reemergence in Greece. Our data sources were countrywide georeferenced environmental and climatic information, all acquired from the European Environment and Epidemiology Network data repository and prepared for spatial modeling (7). Variables considered were temperature, vegetation seasonal variations, altitude, land-cover categories, and demographic indicators. Daytime and nighttime Land Surface Temperature and Normalized Difference Vegetation Index were retrieved from the 1 km–resolution long-term Temporal Fourier transformed imagery from Moderate Resolution Imaging Spectroradiometer (8). Altitude values were derived from the Global Land One-km Base Elevation Digital Elevation Model data from the US Geological Survey Earth Resources Observation Systems data center (<http://eros.usgs.gov>). The coordination of information on the environment (CORINE) land cover from the European Environment Agency provided the framework for land cover patterns exploratory analysis (www.eea.europa.eu/data-and-maps/data/corine-land-cover-2000-clc2000-seamless-vector-database-3). The population density grid of the Joint Research Centre was used as demographic indicator (www.eea.europa.eu/data-and-maps/data/population-density-disaggregated-with-corine-land-cover-2000-1).

The spatial scale for this study was a polygon equivalent to a circular buffer of 3.5 km (40,000 ha). This spatial resolution was considered appropriate to the relatively fine scale at which environmental variability can affect malaria transmission. The construction of the land-cover variables is described in the online Technical Appendix (wwwnc.cdc.gov/EID/article/19/5/12-0811-Techapp1.pdf). A disease risk map was generated by using nonlinear discriminant analysis available in eRiskMapper version 1.1.4 (www.tala.ox.ac.uk) and is described in detail in the online Technical Appendix.

Author affiliations: European Centre for Disease Prevention and Control, Stockholm, Sweden (B. Sudre, M. Rossi, W. Van Bortel, J.C. Semenza); Hellenic Centre for Disease Control and Prevention, Athens, Greece (K. Danis, A. Baka); and National School for Public Health, Athens (N. Vakalis)

DOI: <http://dx.doi.org/10.3201/eid1905.120811>

Table. Environmental suitability mapping of malaria, Greece, 2009–2012*

Variable†	Rank
Digital elevation model	4.4
LST day amplitude 2	5.5
NDVI phase 2	7.0
LST nighttime amplitude 2	7.3
LST nighttime mean	8.1
LST day, maximum	8.1
LST day, mean	8.3
LST day phase 2	8.6
NDVI, maximum	8.7
LST night, maximum	8.9

*Classification of 10 variables average rank (1 to 10) for all bootstrapped cycles. Data sources are as follows: Global 30 Arc-Second Elevation Dataset (GTOPO30), 2005 (<http://eros.usgs.gov>); CORINE Land Cover 2000 seamless vector data, version 15 (Aug 2011), European Environment Agency, 2011 (www.eea.europa.eu/data-and-maps/data/corine-land-cover-2000-clc2000-seamless-vector-database-3); Raster data on population density using CORINE Land Cover 2000 inventory, European Environment Agency, 2009 (www.eea.europa.eu/data-and-maps/data/population-density-disaggregated-with-corine-land-cover-2000-2).

†LST, Land Surface Temperature; NDVI, Normalized Difference Vegetation Index.

The first 10 best ranked variables comprised sea-level altitude and land-surface temperature (Table). Parameters of nighttime and daytime temperatures were predictive in this model; the annual variation (amplitude) and the mean absolute temperature values scored high in the ranking. Predicted suitability of areas for persistent malaria transmission based on these variables are characterized by low elevation; warmer temperatures (which might enable more rapid mosquito and parasite development); and intensive, year-round irrigated agriculture with complex cultivation patterns (generally requiring a high degree of manual labor) (Figure 1). These are probable contributing factors to mosquito presence and, possibly, to malaria transmission.

The accuracy statistics of the bootstrap model revealed a sensitivity of 0.98 (where 1 denotes recognition of all actual presences) and specificity of 0.98 (where 1 denotes recognition of all actual absences). Moreover, historical presence of malaria in Greece, before disease elimination, was extracted from several sources and showed a partially coincident distribution pattern with the suitability map: 41% overlap in Peloponnese, 63% along the west coast of central Greece and Epirus, and 39% in eastern central Greece (Figure 2). The best overlap was found along the west coast, but in the northern part, the model did not match the historical pattern very well. This discrepancy might be explained by the low rank of landscape pattern variables obtained into nonlinear discriminant analysis modeling.

Conclusions

We assessed environmental and climatic characteristics of the areas with autochthonous spread of *P. vivax* malaria in Greece during 2009–2012 and delineated similar areas possibly suitable for transmission in Greece. Sea-level altitude

and the mean and annual variation of land-surface temperature for daytime and nighttime were predictors in our model.

A major limitation of our study is that it considers only environmental suitability for transmission, not risk for transmission per se. Our approach did not account for certain factors in this regard, for example, presence/absence of malaria vectors under collection in 2012. This partly reflects the lack of knowledge about what mosquito species were responsible for recent outbreaks, although historic work suggests *Anopheles sacharovi*, *An. maculipennis s.s.*, and *An. superpictus* (9,10). Indeed, 2 of these species, *An. sacharovi* and *An. superpictus*, have been implicated as the probable dominant vectors throughout Greece and adjacent areas (11). Hence, species would seem to be reasonable targets for any mosquito surveillance efforts.

Our model did not highlight areas of northern Greece previously associated with malaria (4,5) as being particularly suitable for transmission. Further refinement of our approach, perhaps including vector information, might address this shortcoming. Further study on the malariogenic potential should be conducted to complete our assessment. Despite these limitations, this spatial analysis can be useful and can help guide the public health response to threats, such as malaria, by directing surveillance and control activities and/or by identifying uncertainties relevant to disease risk mapping and response.

Model accuracy and public health practice can be improved through vigilant disease and vector surveillance with timely case notification (12). Yet, despite these potential limitations, we believe that this spatial analysis is a useful tool; it can help guide response(s), integrated preparedness and response activities, including targeted epidemiologic and entomologic surveillance, vector control



Figure 1. Areas latently hospitable and environmentally permissive for persistent malaria transmission, Greece, 2009–2012. Map showing areas predicted to be environmentally suitable for malaria transmission. Values from 0 to 0.5 (dark to light green) indicate conditions not favorable for malaria transmission (based on locally acquired cases); yellow to dark red areas delineate conditions increasingly favorable for transmission (values from 0.5 to 1).



Figure 2. Areas of historic malaria transmission before elimination, Greece. Greece was officially declared malaria free in 1974, after a national malaria elimination effort during 1946–1960. Data sources: adapted from (10); Ministry of Health. Map of confirmed laboratory species–1952, unpub. data.

activities, and awareness rising among the general population and health care workers, in the areas environmentally suitable for transmission.

Dr Sudre is a scientific officer environmental determinants of communicable diseases at the European Centre for Disease Prevention and Control in Stockholm and an associate researcher at UMR 6249 Chrono-environnement Laboratory (Besançon, France). His research interests include health geography, as well as eco-epidemiology of infectious diseases and its integration in public health.

References

1. Sabatinelli G, Ejov M, Joergensen P. Malaria in the WHO European Region (1971–1999). *Euro Surveill.* 2001;6:61–5.

2. Danis K, Baka A, Lenglet A, Van Bortel W, Terzaki I, Tseroni M, et al. Autochthonous *Plasmodium vivax* malaria in Greece, 2011. *Euro Surveill.* 2011;16:19993.
3. Vakali A, Patsoula E, Spanakos G, Danis K, Vassalou E, Tegos N, et al. Malaria in Greece, 1975 to 2010. *Euro Surveill.* 2012;17:20322.
4. Kampen H, Maltezos E, Pagonaki M, Hunfeld KP, Maier WA, Seitz HM. Individual cases of autochthonous malaria in Evros Province, northern Greece: serological aspects. *Parasitol Res.* 2002;88:261–6. <http://dx.doi.org/10.1007/s00436-001-0530-2>
5. Kampen H, Proft J, Etti S, Maltezos E, Pagonaki M, Maier WA, et al. Individual cases of autochthonous malaria in Evros Province, northern Greece: entomological aspects. *Parasitol Res.* 2003;89:252–8.
6. Sinka ME, Bangs MJ, Manguin S, Chareonviriyaphap T, Patil AP, Temperley WH, et al. The dominant *Anopheles* vectors of human malaria in the Asia-Pacific region: occurrence data, distribution maps and bionomic precis. *Parasit Vectors.* 2011;4:89. <http://dx.doi.org/10.1186/1756-3305-4-89>
7. Semenza JC, Menne B. Climate change and infectious diseases in Europe. *Lancet Infect Dis.* 2009;9:365–75. [http://dx.doi.org/10.1016/S1473-3099\(09\)70104-5](http://dx.doi.org/10.1016/S1473-3099(09)70104-5)
8. Scharlemann JP, Benz D, Hay SI, Purse BV, Tatem AJ, Wint GR, et al. Global data for ecology and epidemiology: a novel algorithm for temporal Fourier processing MODros Inf Serv. data. *PLoS ONE.* 2008;3:e1408. <http://dx.doi.org/10.1371/journal.pone.0001408>
9. Alten B, Kempen H, Fontenille D. Malaria in southern Europe: resurgence from the past. In Takken W, Knols BGJ, editors. *Emerging pests and vector-borne diseases in Europe.* Wageningen (the Netherlands): Wageningen Academic Publishers; 2007. p. 35–58.
10. Bruce-Chwatt L, Zulueta J, editors. *The rise and fall of malaria in Europe.* New York: Oxford University Press; 1980.
11. Sinka ME, Bangs MJ, Manguin S, Rubio-Palis Y, Chareonviriyaphap T, Coetzee M, et al. A global map of dominant malaria vectors. *Parasit Vectors.* 2012;5:69. <http://dx.doi.org/10.1186/1756-3305-5-69>
12. Lindgren E, Andersson Y, Suk JE, Sudre B, Semenza JC. Public health. Monitoring EU emerging infectious disease risk due to climate change. *Science.* 2012;336:418–9. <http://dx.doi.org/10.1126/science.1215735>

Address for correspondence: Jan C. Semenza, European Centre for Disease Prevention and Control, Unit of Scientific Advice, Tomtebodavägen 11A, Stockholm S-171 83, Sweden; email: jan.semenza@ecdc.europa.eu



Scan this QR Code with your smartphone and enjoy listening to our podcasts about the latest emerging infectious diseases.

<http://wwwnc.cdc.gov/eid/podcasts.htm>



Mapping Environmental Suitability of Malaria Transmission, Greece

Technical Appendix

Description of the Construction on Land-cover Variables

For land cover, variables were constructed by aggregating level 3 CORINE Land Cover classifications (www.eea.europa.eu/data-and-maps/data/corine-land-cover-2000-clc2000-seamless-vector-database-3). Associations of these classifications with malaria data were then assessed through logistic regression by using STATA 10.1-SE (StataCorp LP, College Station, TX, USA) by fitting against the presence/absence of cases. Next, land-cover classifications that were significantly predictive ($p < 10^{-3}$) were pooled to form additional informative layers, representing agricultural and water source patterns. The agricultural layer resulted from an aggregation of different classes, namely fruit trees; berry plantations, and olive groves; land principally occupied by agriculture with significant areas of natural vegetation; and annual crops associated with permanent crops and complex cultivation patterns. Water sources were represented by stagnant water or wetlands, permanently irrigated lands, water bodies, coastal lagoon, estuaries, and salt and inland marshes. Artificial surfaces, forest and seminatural areas classes were not significant and were excluded from further analysis.

Nonlinear Discriminant Analysis

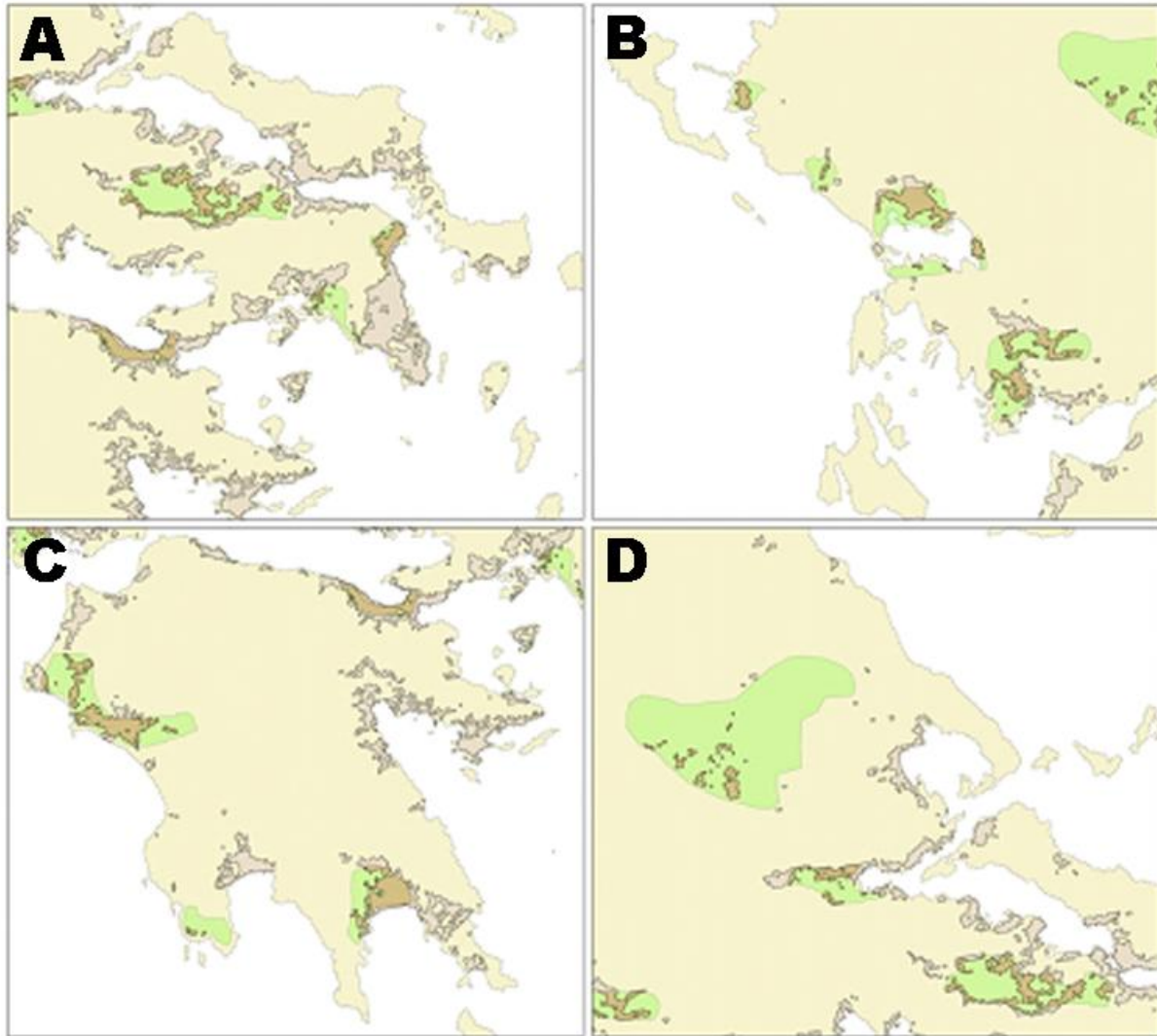
Nonlinear discriminant analysis requires both presence and absence data; however, surveillance data seldom record absences and, if so, seldom in sufficient numbers. “Pseudo-absence” data points must first be generated from the presence data; the models then aim to discriminate between these 2 categories by using the predictor variables available. For the mathematical modeling, besides the 69 domestic malaria case presence points, 210 pseudo-absence points were randomly generated with a minimum distance of 3.5 km from presence points. A disease risk map was generated with these presence and pseudo-absence points, by using nonlinear discriminant analysis (NLDA) available in eRiskMapper version 1.1.4 (www.tala.ox.ac.uk).

Euclidean distance layers from the newly generated landscape classes (distance from agriculture, water sources, and sea coastline) were computed by using ARCGIS Desktop 10 (ESRI, Redlands, CA, USA) and subsequently inputted as additional predictors in NLDA. The NLDA was conducted with 100 bootstrap cycles with 20 replacements for pseudo-absence points in each cycle. To ensure the assumption of multivariate normality of each input variable distribution, clustering was done for absence points by using the best ranked parameters.

Due to the high number of islands in Greece that strongly affect the distribution of the variable “distance-from-coastline,” a sensitivity analysis was performed with and without an islands mask. The pairwise correlation coefficient of a random sample of 20 000 points with a continental location between the 2 models was 0.84 ($p < 10^{-4}$).

Comparison of NLDA and Historical Maps

A comparison between the NLDA and the historical risk maps is hampered by the fact that both maps are probably incomplete and should not be regarded as a gold standard. For a high-resolution visualization, please see the 4 panels in the Technical Appendix Figure.



Technical Appendix Figure. Comparison of the historical map with Athens and East/Central Greece (A); Epirus, East/Central Greece (B); Peloponnese (C); and South Thessaly (D). Light brown, Greece; green, historical area; light violet, NLDA model; deep brown, overlapping areas between historical and nonlinear discriminant analysis model.